Development of a Low Radar Cross Section Antenna with Band-Notched Absorber

Mei, P.; Lin, X.Q.; Yu, Jia Wei; Boukarkar, A.; Zhang, P.C.; Yang, Zi Qiang

Published in:
IEEE Transactions on Antennas and Propagation

DOI (link to publication from Publisher):
10.1109/TAP.2017.2780903

Publication date:
2018

Document Version
Accepteret manuscript, peer-review version

Development of a Low Radar Cross Section Antenna with Band-Notched Absorber

Peng Mei, *Student member, IEEE*, Xian Qi Lin*, *Senior member, IEEE*, Jia Wei Yu, Abdelheq Boukarkar, *Student member, IEEE*, Peng Cheng Zhang, and Zi Qiang Yang#

***Abstract*—A low radar cross section (RCS) antenna designed with band-notched absorber is described. Firstly, a dual-polarization absorber with relative bandwidth more than 80% is designed using loaded-resistors. Pairs of circular slot resonators and metal strip array resonators are introduced in the absorber to realize a notch band with full reflectance in the vertical polarization while a wide absorption band in the horizontal polarization is maintained. The proposed band-notched absorber is thus realized. Within the notch band, the absorber can be served as a metal ground for antenna; while a great RCS reduction is obtained out of the notch band and in the horizontal polarization band. Then, a dipole antenna rigorously designed is mounted above the band-notched absorber, whose operating frequency is exactly in accordance with that of the notch band. The proposed low RCS antenna is established based on assembling the dipole antenna and the band-notched absorber together. The measured results demonstrate that the proposed antenna has fairly good radiation patterns. Added to that, more than 10dB RCS reduction in two polarizations is realized simultaneously compared with that one of a conventional dipole antenna.**

***Index Terms*—Band-notched absorber, radar cross section reduction, notch-band, low RCS antenna.**

I. Introduction

With the rapid development of the stealth and detection technology, radar cross section (RCS) reduction of a target is urgently needed. As a necessary device for the communication on the platform, the antenna does not only radiate electromagnetic wave effectively, but also contribute to the main radar cross section of the aircrafts or other bulky platforms. There are some methods to reduce the antenna RCS, such as shaping [1]-[4], using radar absorber materials (RAMs) [5]-[11], polarization conversion metasurfaces [12]-[14], and artificial magnetic conductor surfaces [15], [16]. The conventional RAMs method to reduce RCS has some negative impacts on the radiation performances of the antenna, such as low radiation gain and poor radiation patterns. As a result, it is challenging to reduce the RCS without degrading the antenna's radiation performances. Moreover, it is much preferable to realize the RCS reduction in a much wider frequency band.

Tracing back to the antenna RCS reduction using RAMs, it is found that the RAMs and antenna are usually designed individually, they are then arranged together on the same plane to reduce the RCS of the extra metal ground. In order not to distort the radiation patterns of the antenna, the RAMs are usually assigned away from the radiation patch or radiation slot to ensure the effective radiation area not to be disturbed [5], [6]. In [5], the authors presented a perfect absorber with fractal techniques, and then they assigned these absorber structures around a patch antenna to realize the RCS reduction. Likewise, the authors in [6] also designed an absorber and waveguide slot antenna operating at the same frequency, they rigorously arranged the absorbers around the slot antenna to realize the RCS reduction. Due to the extremely finite absorption bandwidth of these kinds of resonant structured absorbers, the antenna can only realize low RCS in a narrow bandwidth. Using polarization conversion metasurfaces or artificial magnetic conductors can just decrease the antenna's RCS in a specific angle (θ=0°) by using the out of phase cancellation of these metasurfaces's reflection phases. Based on the energy conservation, the decreased energy in the definite angle is scattered to other angles, which is not applicable for bistatic radar detection in practice. Moreover, this method just realizes RCS reduction in a narrow band as well.

In this paper, we propose a different method to realize a low RCS antenna compared with the previously reported conventional RAMs method [5], [6]. Firstly, a dual-polarization, and wide bandwidth absorber is designed with resistor-loaded. Pairs of circular slot resonators and metal strips resonators are introduced to generate a notch band in the vertical polarization, while the wide absorption performance in the orthogonal polarization is still maintained. Then, a single-polarization dipole antenna as a sample is rigorously designed, whose operating frequency is exactly in accordance with that of the notch band. The reflection phases of the notch band are also noticed to determine the definite location of the dipole antenna to obtain good radiation patterns and radiation

Manuscript received June 19, 2017. This work was supported in part by National Nature Science Foundation of China under Grant 61571084 and Grant 61561021.

The authors are all with the EHF Key Laboratory of Science, School of Electronic Engineering, University of Electronic Science and Technology of China, Chengdu, 611731, China. (*e-mail: xqlin@uestc.edu.cn; #e-mail: yangziqiang@uestc.edu.cn)

Xian Qi Lin is also with the Jiangsu Hengxin Technology Co., Ltd, Wuxi, 214222, China.

gains. Within the notch band, the band-notched absorber can be served as a metal ground for antenna, the antenna works well, radiation patterns of the antenna are fairly good. Out of the notch band, the band-notched absorber is indeed regarded as an absorber, the electromagnetic wave absorption is realized simultaneously, thus, a significant RCS reduction is obtained. The measured results validate the effectiveness of our proposed design, which can be considered as a good reference when designing low RCS antennas.

The paper is organized as follows: In Section II, the dual-polarization, the band-notched absorber, and the dipole antenna are rigorously designed. In section III, the band-notched absorber and dipole antenna are assembled together to realize low RCS. Then, the proposed low RCS antenna with optimal dimensions is fabricated, measured, and discussed in section IV. At last, concluding remarks are drawn in section V.

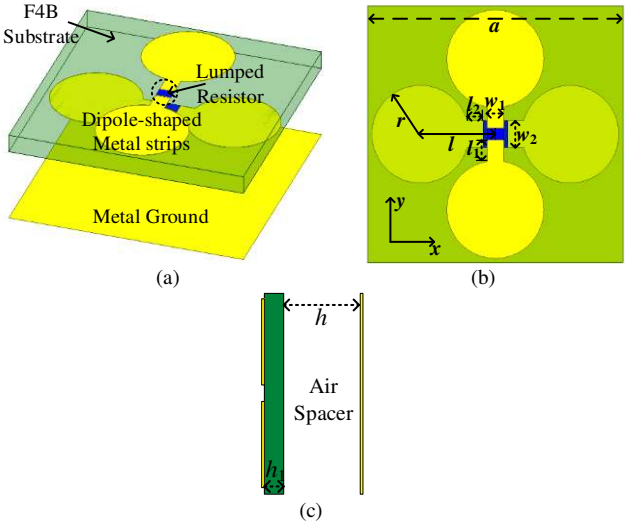

Fig.1. Geometries of the dual-polarization and wide absorption band absorber. (a) Perspective view. (b) Front view. (c) Side view.

II. The Band-Notched Absorber Design Procedure

A. *Dual-polarization, wide absorption bandwidth absorber*

The geometries of dual-polarization and wide absorption bandwidth absorber unit cell is presented in Fig. 1. It consists of an orthogonal dipole-shaped metal strip printing on two sides of the supporting substrate, two lumped resistors, F4B dielectric substrate, an air spacer, and a metal ground. At the vertical polarization, the electric field is in the direction of the *y*-axis, while the electric field in the direction of the *x*-direction is horizontal polarization. The F4B dielectric substrate is used with a thickness of 1mm, a relative permittivity of $\varepsilon_r = 2.65$, and a dielectric loss tangent of $\tan\delta = 0.002$. The lumped resistors are used to realize wide impedance match between the structured absorber and the free space further to obtain wide absorption. The absorption characteristics of the proposed dual-polarization absorber are simulated and analyzed using commercial High Frequency Structure Simulator (HFSS) software. The metal portions in this paper are all modeled as lossy copper with a conductivity $\sigma = 5.8\times10^7\ S/m$.

The impacts of different arrangement statuses of these orthogonal dipole-shaped metal strips on its whole absorption performances are examined. The reflection coefficient of the dual-polarization absorber is checked under three different cases, namely, non-overlap ($l = 3.7mm$), critical condition ($l = 3.4mm$), and overlap ($l = 3.2mm$) with other parameters fixed. The values of the lumped resistors in front and back surfaces of the supporting F4B dielectric substrate are dominated for realizing wide absorption band as studied in [17], [18]. For brevity, we directly assign the front and back resistors with their optimal values 100ohms and 82ohms, respectively. From Fig. 2, two conclusions are obtained: 1). the absorption bandwidth is narrowing when the dipole-shaped metal strips on front and back of the substrate is overlapped; 2). the reflection coefficients in the two polarizations are almost identical. The slight discrepancies are due to the fact that these orthogonal dipole-shaped metal strips are separated by the supporting dielectric substrate. Thus, a non-overlap condition [as shown in Fig. 1(b)] is adopted in our study to achieve wide absorption bandwidth performances.

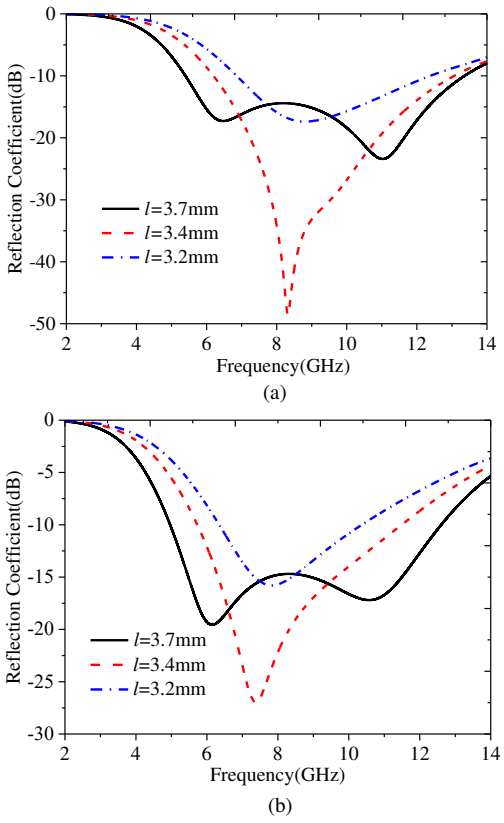

Fig.2. Reflection coefficient under different values of *l*. (a) horizontal polarization. (b) vertical polarization. (a=12.6mm, r=2.4mm, l_1=1.0mm, l_2=0.8mm, w_1=0.8mm, w_2=1.3mm, w_3=0.6mm, w_4=1.2mm, h_1=1mm, h=4mm).

B. Constructing a notch band in the vertical polarization and a wide absorption band in the horizontal polarization

In order to introduce a full reflectance band in the vertical polarization, notch band and FSSs techniques are adopted as described in our previous work [18], The proposed absorber is improved based on Fig. 1 and its geometries is demonstrated in Fig. 3. In the horizontal polarization, the dipole-shaped metal strips in the upper layer and the metal ground in the lower layer together can realize wide absorption performances; while the circular slot resonators in the upper layer and metal strips array in the lower layer generate two independent magnetic resonance and electric resonance, respectively. These magnetic and electric resonances form the notch band in the vertical horizontal polarization.

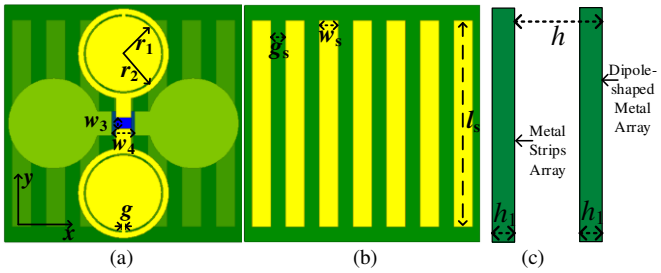

Fig.3. Geometries of the proposed absorber with a notch band in the vertical polarization and a wide absorption band in the horizontal polarization. (a) Perspective view (b) Front view (c) Side view.

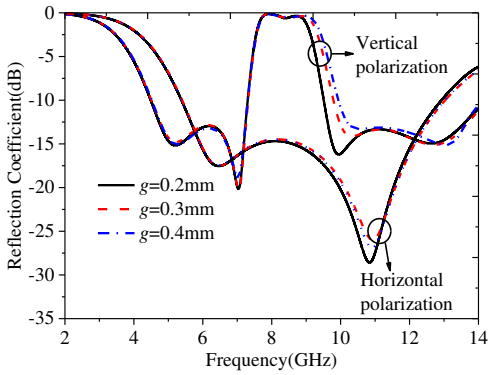

Fig.4. Reflection coefficient under different values of g in two polarizations. (a=12.6mm, r=2.4mm, r_1=2.0mm, r_2=2.1mm, g_s=0.8mm, l=3.7mm, l_1=1.0mm, l_2=0.8mm, l_s= 11.0mm, w_s= 1.0mm, w_1=0.8mm, w_2=1.3mm, w_3=0.6mm, w_4=1.2mm, h_1=1mm, h=4mm).

The notch band with full reflectance will be served as a metal ground for a dipole antenna. As a result, the reflection phase of the notch band is significant to determine the definite location of a dipole antenna to ensure good radiation patterns and radiation gains. In order to accurately obtain the reflection phase of the notch band, a circular slot resonator is etched in the top surface of the F4B substrate as shown in Fig. 3(a).

For an absorber, a low profile is usually preferred. Thus, h is tuned to check its impact on the reflection coefficient in two polarizations as well as the reflection phase of the notch band. The amplitude of reflection coefficient of the proposed absorber can be predicted from ref. [18]. A conclusion that the reflection coefficient performances of the proposed absorber is given directly: a smaller h will deteriorate the performances of the wide absorption in the horizontal polarization; while a larger h will damage the performance of the notch band in the vertical polarization. Here, only the reflection phases of the notch band under different values of h are presented as shown in Fig. 5. According to the reflection coefficients and reflection phases of the notch band, a value of $h = 4mm$ is thus adopted in our design.

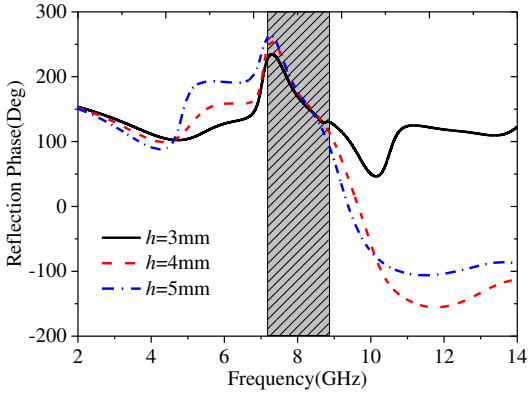

Fig.5. Reflection phase of the notch band with different values of h in the vertical polarization. (a=12.6mm, r=2.4mm, r_1=2.0mm, r_2=2.1mm, g=0.3mm, g_s=0.8mm, l=3.7mm, l_1=1.0mm, l_2=0.8mm, l_s= 11.0mm, w_s= 1.0mm, w_1=0.8mm, w_2=1.3mm, w_3=0.6mm, w_4=1.2mm, h_1=1mm).

III. A Low Radar Cross Section Antenna Designed With Band-Notched Absorber

A. the implementation of low radar cross section antenna with band-notched absorber

In this section, the proposed low RCS antenna that a dipole antenna backed with a band-notched absorber is described. Firstly, the plane absorber with an array of 10 times 10 units as discussed in the previous subsection II. B, is adopted. The dipole antenna rigorously designed is mounted above the array to realize the low RCS antenna. For brevity, only partial geometries of the proposed low RCS antenna are presented in Fig. 6. In order to feed the dipole antenna, a simple balun transition structure is used as shown in Fig. 6(b)-(d). Here, a quadratic function of the envelop of the balun transition is adopted. The design goal of the balun transition is to maintain the characteristic impedance of input port 50ohms and the reflection coefficient at the input port fairly good (at least below -10dB in a certain frequency band). After lots of experimental simulations, we obtained the optimal curve as shown in Fig. 7(b). w_5, l_5 and l_6 are decided simultaneously, and equal to 2.3mm, 15.0mm, and 10.5mm, respectively. We can describe the optimized curve as $x = a \cdot z^2 + b \cdot z + c$, where coefficients a, b, and c are unknown and to be determined. If we choose the

central position of the dipole antenna as the origin of the coordinate axis as shown in Fig. 7(b). The coordinates of points *A, B,* and *C* are (0,1.25), (-5,2), and (-14,5.35), respectively, according to the coordinate axis. After substituting the coordinates into the foregoing function, the coefficients thus are obtained that a=0.01587, b=-0.07063, c=1.25. The specific dimension descriptions of the dipole antenna are depicted in Fig. 6(c)-(d). The arcs in the radiation edge are engraved to improve the reflection coefficient of the antenna.

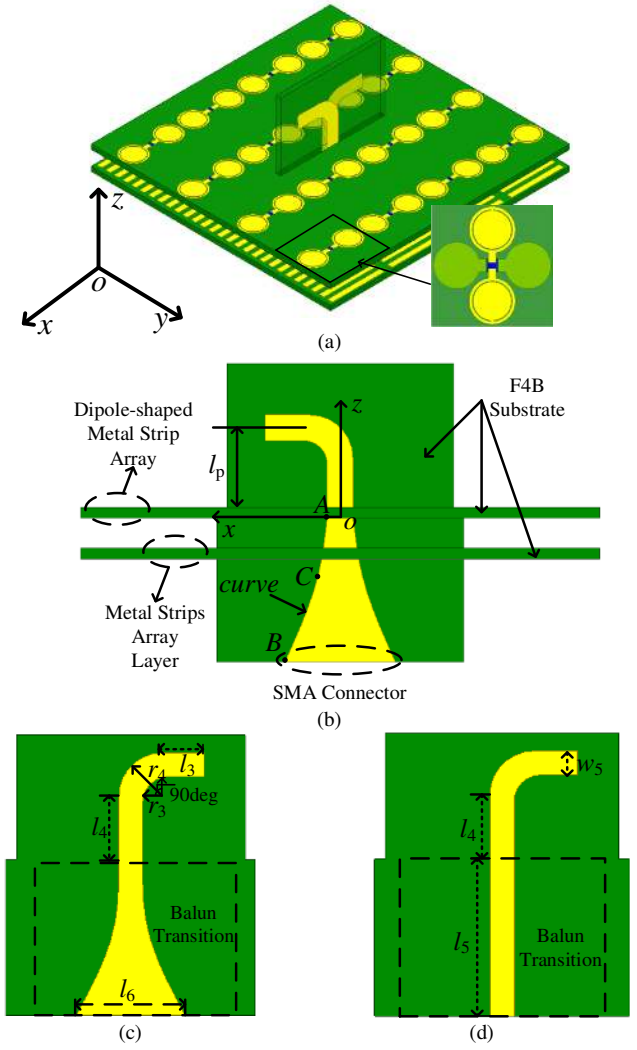

Fig. 6. Geometry of the proposed low RCS antenna. (a) Perspective view. (b) Front view. (c) Front view of dipole antenna. (d) Back view of dipole antenna.

For a dipole antenna backed with a "metal ground", it is widely acknowledged that the separation between the radiation edge of dipole antenna and the so-called metal ground is important to ensure the dipole antenna good radiation patterns and radiation gains. In our case, the distance between the radiation edges of the dipole antenna and the top surface of the band-notched absorber [as shown in Fig. 7(b)] is determined by following equation:

$$-2l_p \times \frac{2\pi f}{c} + \varphi_{Absorber} = 2n\pi, n = 0, \pm1, \pm2, \pm3, \ldots \quad (1)$$

where c is the velocity of free space, f is the interested frequency, $\varphi_{Absorber}$ is the reflection phase of the notch band. Here, the central frequency of the notch band 8.5GHz is selected as the interested frequency. $\varphi_{Absorber}$ is obtained according to the simulated reflection phase of the notch band as shown in Fig. 6. Then, substituting these known values into Eq. (1), the value of l_p is deduced and it equals to 7.5mm. Moreover, once the interested frequency is determined, the length of radiation edge of the dipole antenna is also calculated as follows:

$$2(l_3 + r_3 + w_5) = \frac{c}{\sqrt{2(\varepsilon_r + 1)}f} \quad (2)$$

where ε_r is the relative permittivity of the supporting dielectric substrate.

Additionally, the practical measured reflection phase of the notch band usually has some discrepancies with simulated results due to the fabrication tolerance. According to Eq. (1), l_p is closely related to $\varphi_{Absorber}$, thus, the impacts of different l_p on the proposed low RCS antenna's reflection coefficient is studied with other parameters fixed. Fig. 7 presents the reflection coefficient versus different l_p. It is observed that the impedance bandwidth of the proposed low RCS antenna is stable with different l_p, which means that one still could obtain good radiation pattern and gain at 8.5GHz by simply adjusting the value of l_p even if the reflection phase of the notch band has discrepancy with that of simulated results.

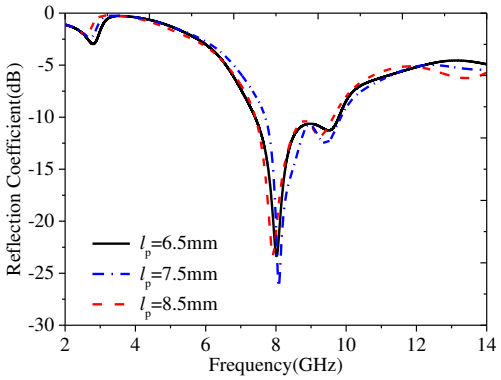

Fig.7. Simulated reflection coefficient of the proposed low RCS antenna versus different l_p. (l_3=4.0mm, l_4=5.5mm, l_5=15.0mm, l_6=10.5mm, r_3=2.5mm, r_4=4.2mm, w_5=2.3mm)

B. Summarized process for the proposed low radar cross section antenna

Based on the above analysis, the design procedures for the proposed low radar cross section antenna can be summed up as the following steps:

1). Specify the shape of the dual-polarization, wide absorption bandwidth absorber; and determine the relative location of the two orthogonal metal strips structure as shown in Fig. 1;

2). According to the interested frequency band, specify the dimension of circular slot resonator etched on top surface of the structure that determined in step (1) and dimension of the metal

strips array in the lower layer as shown in Fig. 3, thus, the band-notched absorber is realized;

3). Specify a dipole antenna mounting above the band-notched absorber designed in step (2) based on the frequencies and reflection phase of the notch band to determine the value of l_p as shown in Fig. 7, where a good reflection coefficient will be obtained.

Tab. I. The optimal dimensions of the proposed low RCS antenna unit (unit: mm)

a	r	r_1	r_2	r_3	r_4	w_1
12.6	2.4	2.0	2.1	2.5	4.2	0.8
w_2	w_3	w_4	w_5	w_s	l_s	h
1.3	0.6	1.2	2.3	1.0	11.0	4.0
h_1	g	g_s	l_1	l_2	l_3	l_4
1.0	0.3	0.8	1.0	0.8	4.0	5.5
l_5	l_6	R_{front}	R_{back}			
15.0	10.5	100ohms	82ohms			

IV. Fabrication, Measurement, and Discussions

A. Fabrication of the proposed low RCS antenna

In this section, the proposed low RCS antenna is fabricated and measured with optimal dimensions as listed in Tab. I. Fig.8 shows the photographs of the proposed low RCS antenna. The metallic patterns of each layer are all etched on F4B substrate. The two layers are attached to each other by the use of four plastic screws placed in the four corners of the dielectric substrates and four at the central part of each side. Plastic screws are also used to keep the two layers parallel at definite distances above each other as shown in Fig. 8. The reflection coefficient of the proposed low RCS antenna is measured by using Agilent vector network analyzer (N5244A), and presented in Fig. 9, where we note that the simulated and measured results are in good agreement.

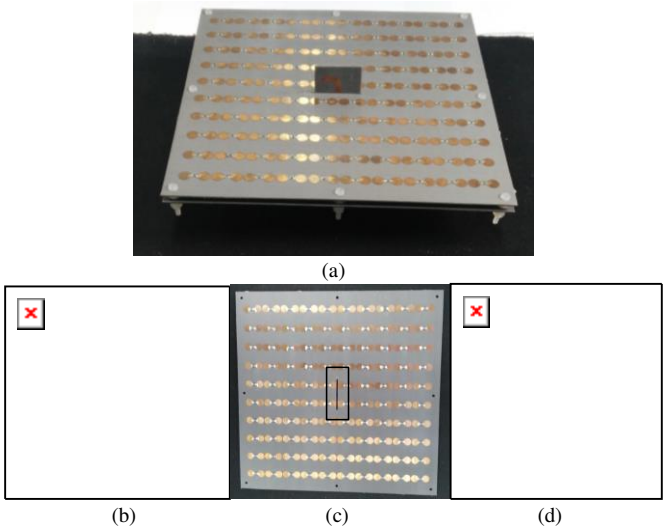

Fig. 8. Photographs of the proposed low RCS antenna. (a). Perspective view. (b). Front view of the upper layer. (c). Back view of the upper layer. (d). Front view of the lower layer.

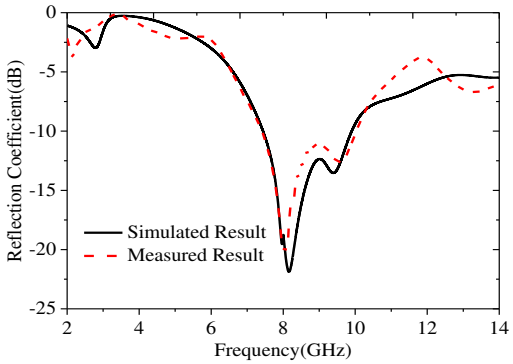

Fig.9. Simulated and measured reflection coefficient of the proposed low RCS antenna.

B. Simulation and measurement of reflection coefficient and radiation patterns

The normalized radiation patterns of the proposed low RCS antenna are also measured to verify its good and stable performances. All the measurements are carried out in our anechoic chamber. Figs. 10 compares the simulated and measured normalized radiation patterns in E- and H-plane at 8.0GHz, and 8.5GHz, respectively. It is observed that the proposed antenna presents stable radiation patterns at these two frequencies, with the main beam pointing toward θ=0°. In the boresight direction, the co-polarization fields of H-plane (*yoz*-plane) and E-plane (*xoz*-plane) are both stronger than their cross-polarization counterparts by about 20dB. The discrepancies of simulated and measured cro-polarization are attributed to misalignment between transmitting antenna and under-test antenna.

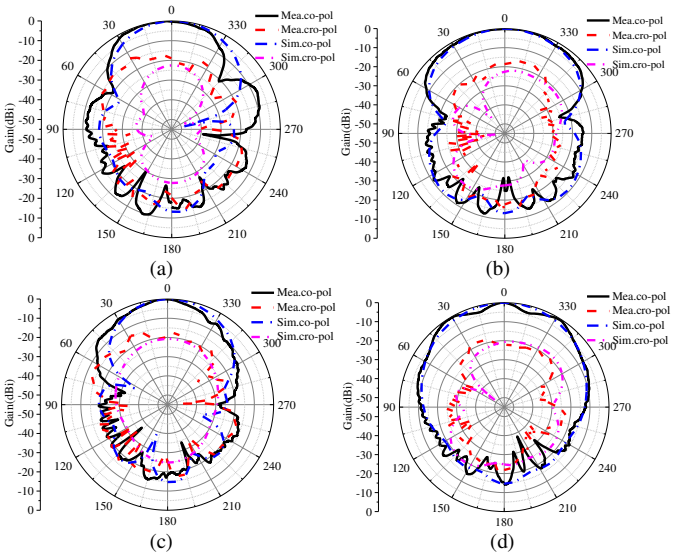

Fig.10. Simulated and measured normalized radiation patterns of the proposed low RCS antenna. (a) E plane ($\varphi = 0^o$) at 8.0GHz. (b) H plane ($\varphi = 90^o$) at 8.0GHz. (c) E plane ($\varphi = 0^o$) at 8.5GHz. (d) H plane ($\varphi = 90^o$) at 8.5GHz.

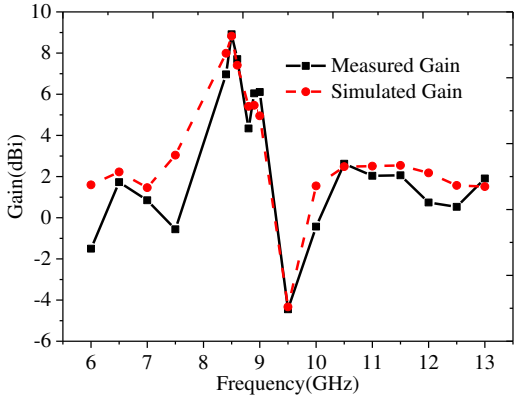

Fig.11. Simulated and measured boresight gains of the proposed low RCS antenna.

Moreover, the boresight gains of the proposed low RCS in a wide band from 5.85GHz to 12.4GHz are also measured. It can be predicted that the gain of the proposed antenna within the notch band is much higher than the gain out of the notch band. As shown in Fig. 11, the boresight gain in the notch band is not stable. This is due to the fact that the reflection phase of the notch band is sharply decreasing when the frequency is increasing, unlike the near 180deg reflection phase of an authentic metal ground in a wide band [19]-[21]. From Fig.11, it is observed that the simulated and measured results have great agreement.

C. *Monostatic radar cross section measurement*

In order to verify the low RCS performance of the proposed antenna, the monostatic RCS at θ=0° of the antenna is measured in two orthogonal polarizations (e.g., horizontal polarization and vertical polarization), where the monostatic RCS of a conventional dipole antenna with identical dimension is also measured for comparison. The measurement setup of monostatic RCS is depicted in Fig. 12. The parabolic antenna is used to convert the spherical wave from transmitting horn antenna to plane wave which directly impinges into the device under test (DUT), the reflective wave from DUT is then propagating into the parabolic antenna and then is received by receiving horn antenna. The vector network analyzer (VNA) processes the transmission and receiving signals to obtain the desired monostatic RCS. In our anechoic chamber, the wide measurement frequency band from 5.85GHz to 12.4GHz is divided into two segments, e.g., from 5.85GHz to 8.17GHz and 8.17GHz to 12.4GHz. This is why there exists a small fluctuation in the measured results at 8.17GHz.

Fig. 13 gives the comparative monostatic RCS results at θ=0° in the horizontal polarization. It is found that a more than 10dB RCS reduction, compared with that one of a conventional dipole antenna working from 5.85GHz to 12.4GHz, is obtained. This can be easily explained from Fig. 4 that the band-notched absorber is exactly served as a wide absorption band absorber in the horizontal polarization in which the antenna does not work.

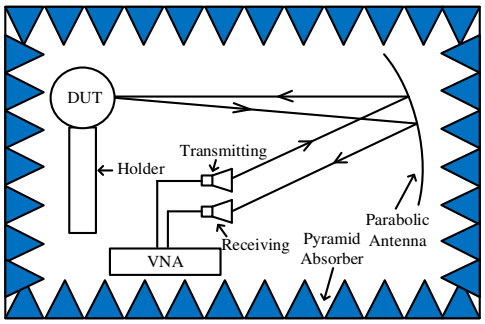

Fig. 12. Measurement setup of monostatic RCS.

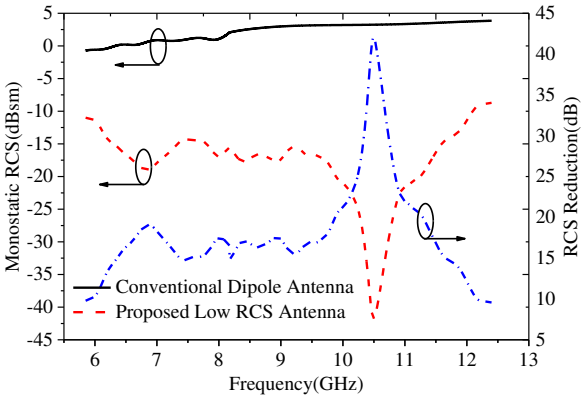

Fig.13. Comparison between the monostatic RCS at θ=0° of a conventional dipole antenna and the proposed low RCS antenna in the horizontal polarization. (These two types of antennas have identical dimensions.)

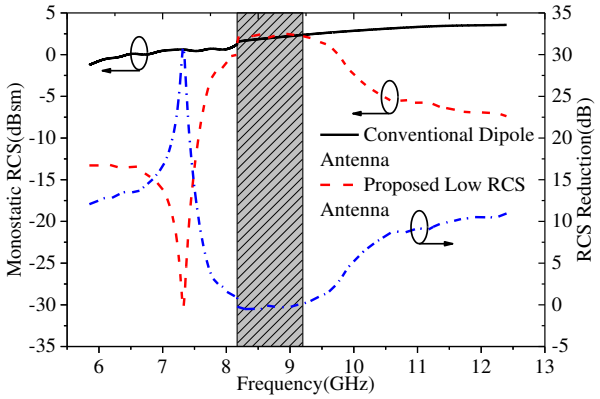

Fig.14. Comparison between the monostatic RCS at θ=0° of a conventional dipole antenna and the proposed low RCS antenna in the vertical polarization (These two types of antennas have identical dimensions.)

In addition, the comparative monostatic RCS results at θ=0° in the vertical polarization are shown in Fig. 14. It is observed that the proposed low RCS antenna and conventional dipole antenna have similar RCS over a definite frequency band (approximately from 8.2GHz to 9.2GHz), which is exactly the operating band of the proposed antenna, while there still exists great RCS reduction out of the notch band. This can also be explained from Fig. 4. In the vertical polarization, the antenna intends to work, and the band-notched absorber is served as an authentic metal ground for the antenna within the notch band,

while it is still regarded as an absorber out of the antenna operating band. As a result, there still exists about 10dB RCS reduction out of the operating band.

V. Conclusion

In conclusion, a low RCS antenna designed with band-notched absorber is described and investigated in detail. A notch band is established by introducing a pair of circular slot resonators and metal strip arrays in the vertical polarization of the dual-polarization wide absorption band absorber unit cell. The frequencies of the notch band can be adjusted by simply tuning the dimensions of the circular slot resonator or metal strip arrays. A dipole antenna is then mounted above the band-notched absorber, whose operating frequency is accordance with that of the notch band. Within the notch band, the antenna works well in the operating polarization, and there still exists a good absorption out of the notch band, while a wide absorption band in the orthogonal polarization is obtained simultaneously. Hence, significant RCS reductions are realized. The proposed low RCS antenna is fabricated and measured. The measured results of reflection coefficient and radiation patterns are in good agreement with simulated results. In addition, the monostatic RCS at θ=0° is also measured. It is shown that more than 10dB RCS reduction is obtained in two orthogonal polarizations.

References

[1] S. Hu, H. Chen, *et al*., "Backscattering cross section of ultrawideband antennas," *IEEE Antennas Wireless Propag. Lett.,* vol. 6, pp. 70-73, 2007.

[2] W. Jiang, Y. Liu, *et al*., "Application of bionics in antenna radar cross section reduction," *IEEE Antenna Wireless Propag. Lett*, vol. 8, pp. 1275-1278, 2009.

[3] Y. B. Thakare, Rajkumar, "Design of fractal patch antenna for size and radar cross section reduction," *IET Microw. Antennas Propag.,* vol. 4, no. 2, pp. 175-181. 2010.

[4] W. Wang, S. Gong, *et al.,* "Differential evolution algorithm and method of moments for the design of low-RCS antennas," *IEEE Antennas Wireless Propag Lett.,* vol. 9, pp. 295-298. 2010.

[5] Y. Liu, X. Zhao, "Perfect absorber metamaterial for deigning low-RCS patch antenna," *IEEE Antennas Wireless Propag Lett.,* vol. 13, pp. 1473-1476. 2014.

[6] Y. Li, H. Zhang, *et al.,* "RCS reduction of ridged waveguide slot antenna array using EBG radar absorbing material," *IEEE Antennas Wireless Propag Lett.,* vol. 7, pp. 473-476. 2008.

[7] T. Liu, X. Cao, *et al.,* "RCS reduction of waveguide slot antenna with metamaterial absorber," *IEEE Trans. Antennas Propag.*, vol. 61, no. 3, pp. 1479-1484. Mar. 2013.

[8] D. Xie, X. Liu, H. Guo, X. Yang, *et al*., "A wideband absorber with a multiresonant gridded-square FSS for antenna RCS reduction," *IEEE Antennas Wireless Propag Lett.,* vol. 16, pp. 629-632. 2017.

[9] Y. Li, H. Zhang, Y. Fu, and N. Yuan, "RCS reduction of ridged waveguide slot antenna array using EBG radar absorbing material," *IEEE Antennas Wireless Propag Lett.,* vol. 7, pp. 473-476. 2008.

[10] H. B. Baskey, E. Johari, and M. J. Akhtar, "Metmaterial structure integrated with a dielectric absorber for wideband reduction of antennas radar cross section," *IEEE Trans. Electromagn. Compat.,* vol. 59, no. 4, pp. 1060-1069, Aug. 2017.

[11] Y. Li, K. Zheng, L. Yang, and L. Du, "Wide-band radar cross-section for antenna using frequency selective absorber," *Electron. Lett*., 2016, vol. 52, no. 21, pp. 1809-1811

[12] Y. Liu, K. Li, *et al.*, "Wideband RCS reduction of a slot array antenna using polarization conversion metasurfaces," *IEEE Trans. Antennas Propag.*, vol. 64, no. 1, pp. 326-331. Jan. 2016.

[13] Y. Liu, Y. Hao, *et al*., "Wideband and polarization-independent radar cross section reduction using holographic metasurface," *IEEE Antennas Wireless Propag Lett.,* vol. 15, pp. 1028-1031. 2016.

[14] Y. Liu, Y. Hao, *et al*., "Radar cross section reduction of a microstrip antenna based on polarization conversion metamaterial," *IEEE Antennas Wireless Propag Lett.,* vol. 15, pp. 80-83. 2016.

[15] Y. Zheng, J. Gao, *et al*., "Wideband RCS reduction of a microstrip antenna using artificial magnetic conductor structures," *IEEE Antennas Wireless Propag Lett.,* vol. 14, pp. 1582-1585. 2015.

[16] Y. Zhao, X. Y. Cao, *et al*, "Broadband RCS reduction and high gain waveguide slot antenna with orthogonal array of polarization-dependent AMC," *Electron. Lett*., 2013, vol. 49, no. 21, pp. 1312-1313.

[17] X. Lin, P. Mei, *et al*., "Development of a resistor-loaded ultra-wideband absorber with antenna reciprocity," *IEEE Trans. Antennas Propag.*, vol. 64, no. 11, pp. 4910-4913. Nov. 2016.

[18] P. Mei, X. Lin, J. Yu, and P. Zhang. "A band-notched absorber designed with high notch-band-edge selectivity," *IEEE Trans. Antennas Propag*. vol. 64, no. 11, pp. 4910-4913. June. 2017.

[19] P. Prakash, M. P. Abegaonkar, A. Basu, and S. K. Koul, "Gain enhancement of a CPW-Fed monopole antenna using polarization-insensitive AMC structure," *IEEE Antennas Wireless Propag Lett.,* vol. 12, pp. 1315-1318. 2013.

[20] J. M. Baracco, L. S. Drioli, and P. D. Maagt, "AMC low profile wideband reference antenna for GPS and GaLILEO systems," *IEEE Trans. Antennas Propag*., vol. 56, no. 8, pp. 2540-2547. Aug. 2008.

[21] W. Yang, K. Tam, W. Choi, W. Che, and H. Hui, "Novel polarization rotation technique based on an artificial magnetic conductor and its application in a low-profile circular polarization antenna," *IEEE Trans. Antennas Propag*., vol. 62, no. 12, pp. 6206-6216. Dec. 2014.

Peng Mei (S'15) was born in Suizhou, Hubei province, China, in 1993. He received the B.Sc. degree in electromagnetic and wireless technology from the University of Electronic and Science Technology of China (UESTC), Chengdu, China, in 2015. He is currently pursuing the M.S degree in electromagnetic filed and microwave technology at UESTC.

His research interests include periodic structure, antenna design, and low radar cross section antenna.

Xian Qi Lin (M'08-SM'15) was born in Zhejiang Province, China, on July 9, 1980. He received the B. S. degree in electronic engineering from the University of Electronic Science and Technology of China (UESTC), Chengdu, China, in 2003, and the Ph.D. degree in electromagnetic and microwave technology from Southeast University, Nanjing, China, in 2008.

He joined the Department of Microwave Engineering, UESTC, in August, and became an Associate Professor and a Doctoral Supervisor in July 2009 and December 2011, respectively. From September 2011 to September 2012, he was a Postdoctoral Researcher in the Department of Electromagnetic Engineering, Royal Institute of Technology, Stockholm, Sweden. He is currently a Full Professor at UESTC. He has authored more than ten patents, more than 40 scientific journal papers, and has presented more than 20 conference papers. His research interests include microwave/millimeter-wave circuits, metamaterials, and antennas.

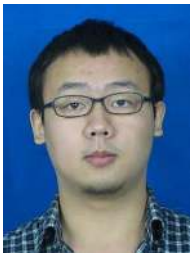

Jia Wei Yu was born in Sichuan Province, China, in March 1991. He received the B.S. degree in electromagnetic and wireless technology from the University of Electronic Science and Technology of China, Chengdu, China, in 2012. He is currently working toward the Ph.D. degree in electromagnetic and microwave technology at UESTC.

His research interests include periodic structure, frequency selective surface, and antenna design.

Abdelheq Boukarkar (S'17) was born in Khenchela, Algeria, in 1984. He received the State Engineering degree in electrical engineering from the École Militaire Polytechnique (EMP), Algiers, Algeria, in 2009, and the M.S. degree from the University of Electronic Science and Technology of China, Chengdu, China, in 2015, where he is currently pursuing the Ph.D. degree in electronic engineering.

His current research interests include antenna design and reconfigurable RF/Microwave circuits.

Peng Cheng Zhang was born in Sichuan Province, China, in 1987. He received the B.S. degree in electromagnetic and wireless technology from the University of Electronic Science and Technology of China (UESTC), Chengdu, China, in 2011. Now, he is pursing the Ph.D. degree in electromagnetic and microwave technology at UESTC.

His interests include antenna design, metamaterial, and microwave/millimeter wave absorber

Zi Qiang Yang was born in Chengdu, Sichuan Province, China, in 1981. He received the B.S. and Ph.D. degrees in electronic engineering from the University of Electronic Science and Technology of China (UESTC), Chengdu, China, in 2003 and 2008, respectively.

In August 2008, he joined UESTC as a Lecturer, and became an Associate Professor in July 2009. From January 2013 to January 2014, he was a Visiting Scholar with the Department of Electrical Engineering, Columbia University, New York, U.S.A. He has authored over 30 scientific journal papers and over 10 conference papers. His present research interests include Microwave monolithic integrated circuits (MMICs), microwave passive components, antennas, and metamaterials.